APL25-AR-02509

Controlled polarity-inversion in GaAs/Ge/GaAs{111} heterostructures

Akihiro Ohtake[1, a)] and Yusuke Hayashi[1]

National Institute for Materials Science (NIMS), Tsukuba 305-0044, Japan

(Dated: 1 May 2025)

We have fabricated the GaAs/Ge/GaAs heterostructures on the {111}-oriented substrates using molecular-beam epitaxy for quasi-phase matching applications in nonlinear optics. The nonlinear optical coefficient of GaAs is beyond that of conventional $LiNbO_3$, enabling more efficient generation of entangled photon pairs via parametric down conversion. We show that GaAs films with either (111)A or (111)B orientation could be grown on the Ge/GaAs{111} substrates, regardless of the polarity of the initial substrates; the (111)A- and (111)B-oriented GaAs overlayers were grown when the surfaces of Ge interlayers on the GaAs{111} substrates were terminated with 1 monolayer (ML)-Ga and 1 ML-In, respectively. Both (111)A- and (111)B-oriented GaAs overlayers have atomically flat surfaces and are almost free of defects, such as rotational twins and stacking faults. The present results provide a promising way to improve the efficiency of nonlinear optical processes in quasi-phase matching devices.

[a)]Electronic mail: OHTAKE.Akihiro@nims.go.jp

III-V semiconductors, such as GaAs and AlAs, are promising materials for nonlinear optical devices, because their nonlinear susceptibilities are significantly higher than those of conventional nonlinear optical crystals, e.g. β-BaB_2O_4, $LiNbO_3$ and $LiTaO_3$.[1–6] Phase matching is essential to realize nonlinear optical effects such as wavelength conversion, where the phase velocities of the excitation and conversion light must be identical. β-BaB_2O_4, which is most commonly used for deep ultraviolet generation, uses birefringence for phase matching by changing the angle of incidence of the excitation light. $LiNbO_3$ uses ferroelectricity to overcome weak birefringence for phase matching by periodically inverting the crystal polarity. This structure is called quasi-phase matching (QPM), because the phase velocity mismatch is compensated by periodically reversing the sign of the nonlinear optical coefficient.[7] Owing to the lack of remarkable birefringence and ferroelectricity in III-V semiconductors, a variety of QPM structures have been developed to overcome the material-related constraints. Examples are periodical polarity inversion[8,9] and vertical polarity inversion[10–13] using well-established technology for crystal growth and device fabrication.

Molecular-beam epitaxy (MBE) has received increased attention for the fabrication of such structures, because of its superiority in controlling the thickness and composition of epitaxial films. This letter reports the fabrication of polarity-inverted structure of GaAs{111} using MBE. To achieve the polarity inversion, thin Ge films were used as interlayers. Since Ge (a=0.56754 nm) and GaAs (a=0.56538 nm) have nearly the same lattice constant (mismatch=0.38 %) and their thermal expansion coefficients are quite close (5.73×10^{-6} K^{-1} for GaAs and 5.90×10^{-6} K^{-1} for Ge), their interface is expected to be coherent and free of defect. Although the fabrication of GaAs/Ge/GaAs heterostructures on the {113}-[14] and {111}-oriented[15] GaAs substrates have been reported earlier, polarity-inverted structures are formed only on the (113)B and (111)A substrates, and the (113)B/Ge/(113)A and (111)A/Ge/(111)B structures have not been realized[14,15]. Here, we show that GaAs films with either (111)A- or (111)B-orientation could be grown on the Ge/GaAs{111} substrates, regardless of the polarity of the initial GaAs substrates. The polarity of MBE-grown GaAs overlayers was identified on the basis of the surface characterization using electron diffraction and scanning tunneling microscopy (STM). We found that the polarity of GaAs overlayers is controlled by the surface treatments for the Ge interlayers on the GaAs{111} substrates: when the surface of the Ge/GaAs{111} substrate is terminated with 1 monolayer (ML) of Ga, the GaAs overlayers show a (2×2) surface reconstruction, characteristic of the (111)A surface. On the other hand, the GaAs overlayers grown on the Ge interlayers terminated with 1 ML of In show ($\sqrt{19}\times\sqrt{19}$)-like surface reconstructions, providing the evidence for the (111)B-

oriented growth. In addition, we show that the formation of twin defects in both (111)A- and (111)B-oriented GaAs overlayers is effectively suppressed. The present growth technique makes it possible to successively grow alternating (111)A and (111)B layers of GaAs. This is expected to increase the conversion efficiency of nonlinear optical processes.

The growth experiments were carried out using a multi-chamber MBE system.[16] The system is equipped with STM and X-ray photoelectron spectroscopy (XPS) apparatuses for online characterization. The clean surfaces of GaAs(111)A-(2×2) and (111)B-($\sqrt{19}\times\sqrt{19}$)-R23.4° were first prepared by MBE.[17] Thin Ge films were grown on the GaAs{111} substrates at 450°C and were subsequently annealed at 550°C. The growth rate of Ge was approximately 0.015 bilayer (BL)/s, which was calibrated by using intensity oscillations of reflection high-energy electron diffraction (RHEED) measurements on the (001)-oriented Ge substrate. Here, 1 BL of Ge is defined as 1.4×10^{15} atoms/cm^2. The GaAs films were grown on the Ge films on GaAs substrates at 450∼650°C with an As_4/Ga flux ratio ranging from 50 to 125. The growth rate was 0.02 BL/s (1 BL of GaAs{111} consists of 1 ML of As and 1 ML of Ga.

The growth processes were monitored by in situ RHEED with an electron-beam energy of 15 keV. The samples were also characterized by online STM, XPS, and low-energy electron diffraction (LEED). All the STM images were collected at room temperature (RT) in the constant current mode with a tunneling current of 0.1 nA and sample voltages between $-1.7\sim-3.0$ V. XPS measurements were performed using monochromatic Al Kα radiation (1486.6 eV). Photoelectrons were detected at an angle of 35° from the surface. The LEED patterns were recorded at RT using primary electron-beam energies ranging from 30 to 200 eV. We obtained LEED patterns at eight locations across the sample, and confirmed the uniformity of the surface structures.

The fabrication of GaAs/Ge/GaAs heterostructures consists of two main steps: the preparation of thin and uniform Ge interlayers on GaAs{111} substrates and the polarity-controlled growth of GaAs overlayers on Ge interlayers. Fisrt, since no systematic studies have been reported for the polarities of GaAs on Ge(111), we carried out the growth experiments of GaAs on bulk Ge(111) substrates to establish the growth procedures for the polarity-controlled GaAs overlayers. The Ge(111) surfaces were prepared by growing undoped buffer layers (50 BL-thick) on thermally cleaned Ge(111) substrates. In an attempt to control the polarity of the GaAs films, the Ge(111) surfaces were terminated with 1 ML of Ga (a) or As (b), prior to the growth of the GaAs overlayers. It has been reported that the As- and Ga-terminated Ge(111) surfaces have atomic structures in which the outermost Ge atoms of the ideal Ge(111) surface are replaced by As[18] and Ga[19] atoms,

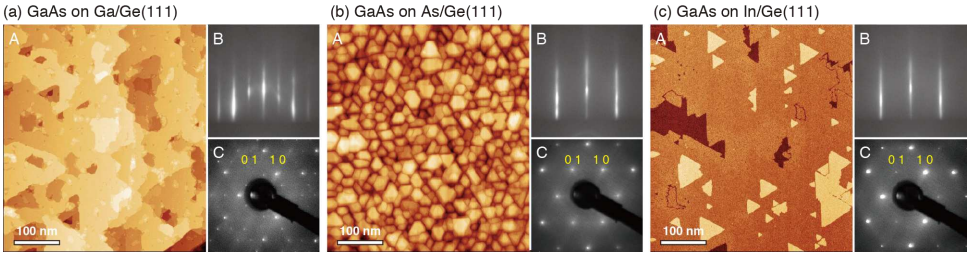

FIG. 1. Typical filled-state STM images (A) of 10 BL-GaAs films grown on bulk Ge(111) substrates terminated with 1 ML of Ga (a), As (b), or In (c), and the corresponding RHEED (B) and LEED (C) patterns. The STM images were taken with a bias voltage of -3.0 V. Image dimensions are 500 nm $\times$ 450 nm. RHEED patterns were taken along the $[\bar{1}01]$ direction of the Ge(111) substrate. LEED patterns were taken at 178 eV (a) and 184 eV (b and c).

respectively. It was therefore expected that the (111)B- and (111)A-oriented GaAs films would grow on the As- and Ga-terminated Ge surfaces, respectively, similarly to the case for GaAs on As/Si(111).[20]

The GaAs film on the As-terminated Ge substrate was grown at 550°C with an As_4/Ga flux ratio of $\sim$70, whereas the film on the Ga-terminated Ge substrate was grown at 450°C with an As_4/Ga flux ratio of $\sim$120. As shown in Figs. 1(a)-B and 1(b)-B, the surfaces of the growing GaAs films on the Ga- and As-terminated Ge(111) substrates show (2$\times$2) and (1$\times$1) RHEED patterns, respectively, from the beginning of the growth ($>$ 1 BL thickness). While only a Ga-rich (2$\times$2) reconstruction is observed on the MBE-grown GaAs(111)A surface,[21] under conventional MBE conditions, ($\sqrt{19}\times\sqrt{19}$) and (1$\times$1) structures are observed on the (111)B surface.[21,22] Thus, it is likely that the GaAs films are grown with the (111)A and (111)B orientations on the Ga-terminated and As-terminated Ge substrates, respectively, as expected.

Figures 1(a) and 1(b) show typical filled-state STM images of 10 BL-GaAs films grown on the Ga- and As-terminated Ge(111) substrates, respectively. The GaAs films grown on the As-terminated substrate consists of small islands; the majority of them have triangular and hexagonal shapes. The LEED pattern (inset in Fig. 1(b)) shows a sixfold symmetry, irrespective of the incident electron energy, indicating the formation of rotational twin domains. On the other hand, the GaAs films on the Ga-terminated substrate have a threefold symmetry (insets in Fig. 1(a))

and shows a rather flat surface morphology: the surface has a smaller root-mean-square roughness (R_q) value of 0.35 nm, as compared with that grown on the As-terminated substrate (1.27 nm).

Previous studies have shown that the GaAs growth on Ge(111) usually is accompanied by the formation of rotational twins.[23,24] The existence of twin domains potentially induces optical scattering and reduces carrier mobilities at the domain boundaries; it is therefore undesirable for device applications. As we will show below, the formation of twins in the (111)B-oriented film was greatly suppressed when the initial Ge surface was terminated with 1 ML-In. The growing surface shows (1×1) RHEED patterns from the beginning of the growth, suggesting the onset of the (111)B-oriented growth. As shown in Fig. 1(c), the surface morphology is highly improved (R_q=0.140 nm), and the formation of rotational twins is effectively suppressed, as can be seen from the threefold LEED pattern.

It is interesting to note that the In and Ga, both being group III elements, induce the GaAs growth with opposite polarities. Previous studies have shown that In- and Ga-terminated Ge(111) surfaces have similar atomic structures.[19] On the other hand, it has been reported that the inter-diffusion occurs at the GaAs/Ge(111) interface.[25] This suggests that the Ga- and In-terminated Ge(111) structures are not preserved at the GaAs/Ge interface, and that the complex atomic rearrangement occurs at the interface.

The next step in achieving the polarity-controlled GaAs/Ge/GaAs heterostructures is to obtain flat and uniform Ge thin layers on GaAs{111} substrates. The STM images and corresponding LEED patterns for 10 BL-Ge films grown on the GaAs(111)A-(2×2) and (111)B-($\sqrt{19}\times\sqrt{19}$) substrates are shown in Fig. S1 in the supplementary material. The Ge surfaces prepared on the (111)A and (111)B substrates have similar R_q values of 0.173 nm and 0.178 nm, respectively, whereas a slight difference was observed in step morphologies between the two surfaces. The corresponding LEED patterns clearly show a threefold symmetry, indicating that rotational twin domains are hardly formed in the Ge films.

Having established the growth procedures for Ge interlayers and GaAs overlayers, we are now in a position to fabricate polarity-controlled GaAs/Ge/GaAs{111} heterostructures. Figures 2(a)-2(d) show a series of RHEED patterns observed during the fabrication of the heterostructure on the (111)A substrates. GaAs films were grown on the 10 BL-Ge layers on the GaAs substrates under conditions otherwise identical to those for GaAs on bulk Ge. Prior to the growth of the GaAs overlayers, the surface of 10 BL-Ge(111) layers was terminated with 1 ML of Ga. The growing GaAs films show (2×2) RHEED patterns (Fig. 2(c)), indicating the formation of a

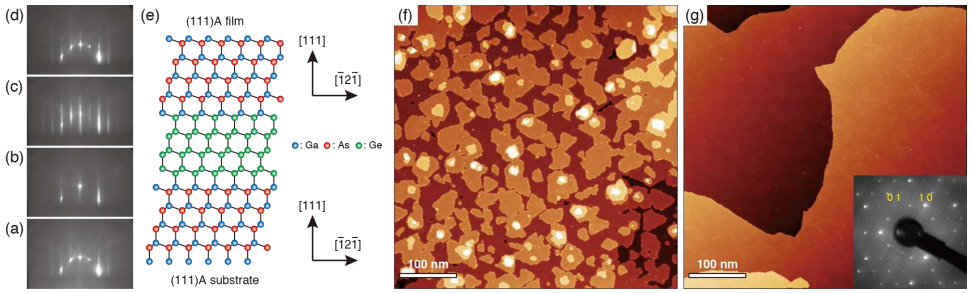

FIG. 2. RHEED patterns taken during the growth of GaAs/Ge/GaAs heterostructures grown on the (111)A-oriented substrates: (a) the initial (111)A-(2×2) surface, (b) the 10 BL-Ge film, (c) as-grown 10 BL-GaAs film, and (d) 30 BL-GaAs film after annealing at 650°C. The electron-incidence azimuth is [$\bar{1}$01]. The RHEED pattern changes from (a) to (d) in an upward direction as the growth proceeds. (e) shows a schematic drawing of the heterostructure. (f) and (g) show STM images taken with a bias voltage of −3.0 V from the as-grown 10 BL-thick GaAs film and the 30 BL-thick GaAs film after annealing at 650°C, respectively. Image dimensions are 500 nm×500 nm. The inset in (g) shows the corresponding LEED pattern taken from the surface (178 eV).

GaAs(111)A/Ge/GaAs(111)A heterostructure, as shown in Fig. 2(e). Figure 2(f) shows a filled-state STM image from the 10 BL-thick GaAs films grown at 450°C; two-dimensional islands are observed (R_q=0.28 nm). The density of the islands are significantly decreased after the annealing at 650°C under the As flux, resulting in the improved surface morphology (R_q=0.16 nm) (see Fig. S2 in the supplementary material). The additional 20 BL-growth and the subsequent annealing at 650°C further improved the surface morphology, as shown in Fig. 2(g) (R_q=0.14 nm). The RHEED pattern shown in Fig. 2(d) is quite similar to that of the initial GaAs(111)A substrate (Fig. 2a), indicating that the overgrown GaAs film has the same orientation as the GaAs substrate.

To promote the GaAs growth with the reversed orientation of (111)B, the surface of the Ge interlayers was terminated with 1 ML of In. Figures 3(a)-3(d) show RHEED patterns observed during the growth on the Ge/GaAs(111)A substrate. The surface of the growing GaAs overlayer shows very weak ($\sqrt{19}\times\sqrt{19}$) RHEED patterns, indicating the formation of polarity-inverted GaAs(111)B layers on the Ge/GaAs(111)A substrate (Fig. 3(e)). Although the optimum temperature for the (111)B growth is 650°C,[17] the first 10 BL-GaAs film was grown at a lower temperature

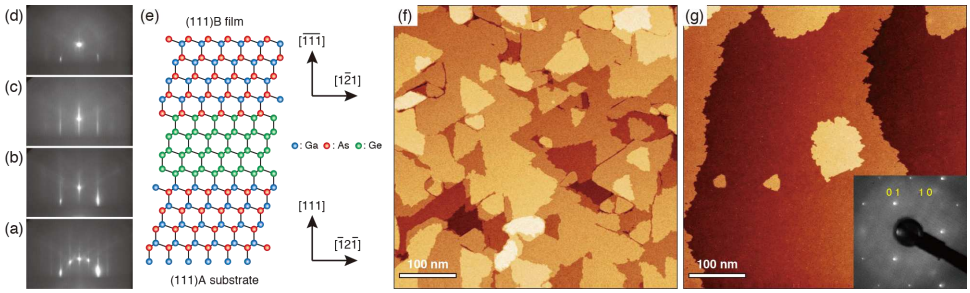

FIG. 3. RHEED patterns taken during the growth of GaAs/Ge/GaAs heterostructures grown on the (111)A-oriented substrates: (a) the initial (111)A-(2×2) surface, (b) the 10 BL-Ge film, (c) as-grown 10 BL-GaAs film, and (d) 30 BL-GaAs film after annealing at 650°C. The electron-incidence azimuth is [$\bar{1}$01]. The RHEED pattern changes from (a) to (d) in an upward direction as the growth proceeds. (e) shows a schematic drawing of the heterostructure. (f) and (g) show STM images taken with a bias voltage of −3.0 V from the as-grown 10 BL-thick GaAs film and the 30 BL-thick GaAs film after annealing at 650°C, respectively. Image dimensions are 500 nm×500 nm. The inset in (g) shows the corresponding LEED pattern taken from the surface (169 eV).

of 550°C to suppress the possible desorption of In during the growth. The low-temperature growth results in a slightly degraded surface morphology, as can be seen in Fig. 3(f) (R_q=0.273 nm), because the surface diffusion of Ga atoms is less enhanced. Similarly to the case for the (111)A growth, the R_q value is decreased to 0.196 nm after the annealing at 650°C, and the subsequent 20 BL-growth at 650°C further improves the surface morphology (R_q=0.158 nm), as shown in Fig. 3(g).

The polarity inversion of GaAs(111)B on Ge/GaAs(111)A was also confirmed by high-angle annular dark-field scanning transmission electron microscopy (HAADF-STEM) and energy dispersive x-ray spectroscopy (EDX). As shown in Fig. 4(a), both the GaAs/Ge and Ge/GaAs interfaces are coherent and the GaAs(111)B films are free of defects. The magnified STEM image (Fig. 4(b)) and atomically-resolved EDX image (Fig. 4(c)) clearly show that the GaAs films were grown with the (111)B orientation on the Ge interlayers (see also Fig. S3 in the supplementary material).

We carried out the growth experiments on the GaAs(111)B substrate, and confirmed that

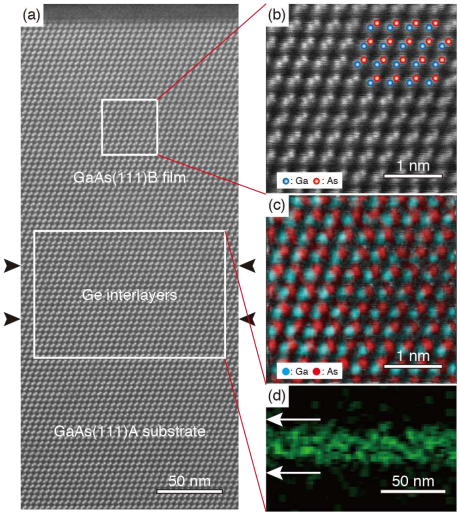

FIG. 4. (a) HAADF-STEM image of the polarity-inverted GaAs(111)B/Ge/GaAs(111)A heterostructure. The nominal thickness of GaAs films is 50 BL. Arrowheads indicate the positions of the GaAs/Ge and Ge/GaAs interfaces. (b) Magnified STEM image. (c) Atomically-resolved EDX image of the region (b) with the Ga-K (blue) and As-K (red) lines. (d) EDX image of the Ge interlayers with the Ge-K line (green). Horizontal arrows indicate the positions of the interfaces.

polarity-controlled heterostructures are also formed on the (111)B substrate (see Fig. S4 in the supplementary material). On both substrates, the growth temperature (450°C for (111)A, and 550°C and 650°C for (111)B) is an important factor in determining the crystal quality of the overgrown GaAs film: (111)A-oriented GaAs films grown at 550°C gives rise to a degraded surface morphology with the formation of rotational twins. Similarly, the successive growth of GaAs(111)B ($>$ 10 BL) at 550°C results in the degradation of the surface morphology and the formation of rotational twins.

Figure 5(a) shows the STM image taken from the 30 BL-GaAs film grown on the Ga-terminated Ge layers on GaAs(111)A. A (2×2) periodicity is clearly seen, corresponding to the Ga-vacancy buckling structure (inset in Fig. 5(a)).[26,27] Figure 5(c) shows LEED $I-V$ curves for the 1 0 and 0 1 beams measured from the 30 BL-GaAs films (red curves). Also shown are $I-V$ curves measured from the (2×2) surface on bulk GaAs(111)A (blue curves). An excellent agreement between the

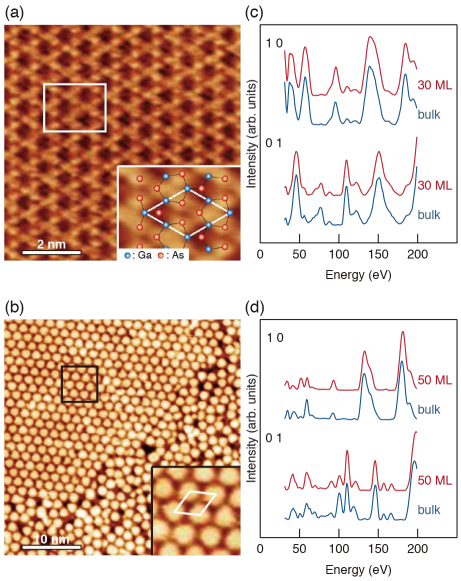

FIG. 5. Typical STM images of the 30 BL-GaAs films grown on the Ga-terminated Ge layers (a) and 100 BL-GaAs films grown on the In-terminated Ge layers (b) on the GaAs(111)A substrates. Image dimensions are 8 nm×8 nm and 40 nm×40 nm, respectively. The images (a) and (b) were taken with bias voltages of -1.7 V and -3.0 V, respectively. The insets in (a) and (b) show the magnified images with dimensions of 1.6 nm×2.1 nm and 6 nm×6 nm, respectively. (c) LEED $I-V$ curves measured from the (111)A-(2×2) surfaces of 30 BL-GaAs (red curves) and bulk GaAs (blue curves). (d) LEED $I-V$ curves measured from the (111)B-($\sqrt{19}\times\sqrt{19}$) surfaces of 50 BL-GaAs (red curves) and bulk GaAs (blue curves).

two curves further confirms that the overgrown GaAs film has a (111)A orientation. The measured $I-V$ curves are well reproduced by the calculations for the Ga-vacancy buckling model (see Fig. S5 in the supplementary material).

Shown in Fig. 5(b) is the magnified STM image observed from the thick GaAs film (100 BL) grown on the In-terminated Ge film (10 BL) on GaAs(111)A. There exist ordered and disordered regions, and bright spots are arranged with a ($\sqrt{19}\times\sqrt{19}$) periodicity in the ordered region (inset of Fig. 5(a)), indicating the formation of the (111)B surface. Further evidence for the (111)B orientation was obtained from the LEED measurements: as shown in Fig. 5(d), LEED $I-V$

curves measured from the 50 BL-thick GaAs films (red curves) and the $(\sqrt{19}\times\sqrt{19})$ surface of bulk GaAs(111)B (blue curves) are quite similar.

Figures 6(a)-6(f) show magnified STM images of GaAs(111)B overlayers with various film thicknesses grown on the Ge/GaAs(111)A substrate. The density of bright spots in STM images, corresponding to the hexagonal rings in the $(\sqrt{19}\times\sqrt{19})$ structure,[28] is below 50% at the early stage of the growth, and is increased as the growth proceeds. This means that the $(\sqrt{19}\times\sqrt{19})$ structure is incomplete on thinner GaAs(111)B films. As mentioned earlier, it has been reported that the interdiffusion occurs at the GaAs/Ge(111) interface.[20] As shown in Fig. 6(h), our XPS measurements show that the Ge 3d signal could be clearly seen in the spectrum measured from the 20 BL-GaAs(111)B film (B), whereas the Ge intensity for the 20 BL-GaAs(111)A film was one order of magnitude smaller (A), suggesting that there was greater interdiffusion at the GaAs(111)B/Ge(111) interface. Therefore, it is plausible to consider that Ge atoms are incorporated in thinner GaAs(111)B films growing at relatively high temperatures of 550°C and 650°C, which disturbs the formation of the $(\sqrt{19}\times\sqrt{19})$ structure. As the film thickness increases, the number of Ge atoms in the GaAs film decreases because of the kinetic limitation of the diffusion, leading to pure GaAs(111)B growth with a $(\sqrt{19}\times\sqrt{19})$ surface. The change in the surface structure of the GaAs(111)B film is also observed in LEED $I-V$ curves: the shape of the $I-V$ curves measured from the (111)B film strongly depends on the film thickness, whereas no noticeable change was observed for the (111)A film, as shown in Fig. S6 in the supplementary material.

In conclusion, we studied the polarity of MBE-grown GaAs{111} films on Ge/GaAs{111} substrates using complementary experimental techniques of RHEED, LEED, and STM. The insertion of thin Ge interlayers enables us to control the polarity of GaAs overlayers in GaAs/Ge/GaAs{111} heterostructures: the (111)A-oriented GaAs films are grown when the surface of Ge layers is terminated with 1 ML of Ga, while the termination with 1 ML of In leads to the (111)B-oriented GaAs growth. The present results are expected to increase the efficiency of GaAs-based QPM nonlinear optical devices. This technique also opens attractive possibilities for the generation of entangled photon pairs via parametric down conversion.

See supplementary material for the STM results of Ge films (Fig. S1), additional RHEED and STM results (Figs. S2 and S4), HAADF-STEM and EDX images (Fig. S3), LEED I-V curve analysis for the (111)A-(2×2) surface (Fig. S5 and Table S1), and LEED I-V curves for GaAs(111)A and (111)B films with various thicknesses (Fig. S6).

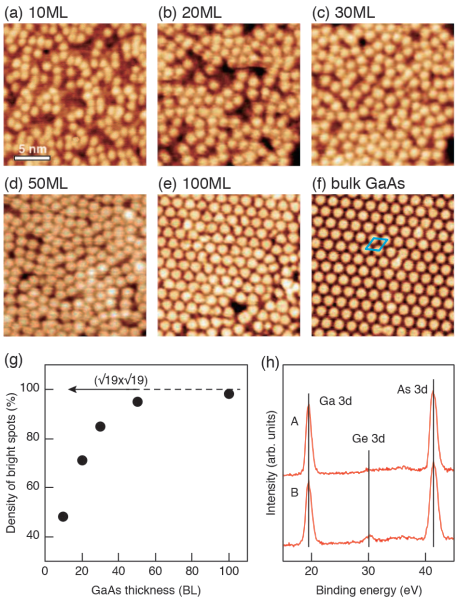

FIG. 6. STM images of the GaAs(111)B films with a bias voltage of -3.0 V (a-f). Image dimensions are 20 nm$\times$20 nm. The $(\sqrt{19}\times\sqrt{19})$ unit cell is indicated in (f). (g) shows the densities of bright spots in STM images plotted as a function of the GaAs film thickness. (h) XPS spectra of Ga 3d, Ge 3d and As 3d. The spectrum A (B) was obtained from the 20 BL-GaAs(111)A (GaAs(111)B) film on the Ga- (In-) terminated Ge layers.

ACKNOWLEDGMENTS

Helpful discussions with Dr. T. Mano are gratefully acknowledged.

AUTHOR DECLARATIONS

Conflict of Interest

The authors have no conflicts to disclose.

Author Contributions

Akihiro Ohtake: Conceptualization (lead); Data curation (lead); Formal analysis (lead); Investigation (lead); Methodology (lead); Writing – original draft (lead); Writing – review & editing (lead). **Yusuke Hayashi**: Conceptualization (equal); Writing – review & editing (supporting)

DATA AVAILABILITY

The data that support the findings of this study are available from the corresponding author upon reasonable request.

REFERENCES

[1]I. Shoji, H. Nakamura, K. Ohdaira, T. Kondo, R. Ito, T. Okamoto, K. Tatsuki, and S. Kubota, Absolute measurement of second-order nonlinear-optical coefficients of β-BaB_2O_4 for visible to ultraviolet second-harmonic wavelengths J. Opt. Soc. Am. B **16**, 620-624 (1999).

[2]I. Shoji, T. Kondo, and R. Ito, Second-order nonlinear susceptibilities of various dielectric and semiconductor materials, Opt. Quantum Electron. **34**, 797-833 (2002).

[3]S. Buckley, M. Radulaski, J. Petykiewicz, K. G. Lagoudakis, J.-H. Kang, M. Brongersma, K. Biermann, and J. Vučković, Second-Harmonic Generation in GaAs Photonic Crystal Cavities in (111)B and (001) Crystal Orientations, ACS Photonics **1**, 516-523 (2014).

[4]L. Chang, A. Boes, P. Pintus, J. D. Peters, M. Kennedy, X.-W. Guo, N. Volet, S.-P. Yu, S. B. Papp, and J. E. Bowers, Strong frequency conversion in heterogeneously integrated GaAs resonators, APL Photonics **4**, 036103 (2019).

[5]E.J. Stanton, J. Chiles, N. Nader, G. Moody, N. Volet, L. Chang, J.E. Bowers, S. Woo Nam, and R.P. Mirin, Efficient second harmonic generation in nanophotonic GaAs-on-insulator waveguides, Opt. Express **28**, 9521-9532 (2020).

[6]M. Placke, J. Schlegel, F. Mann, P. Della Casa, A. Thies, M. Weyers, G. Tränkle, and S. Ramelow, Telecom-band spontaneous parametric down-conversion in AlGaAs-on-insulator waveguides, Laser Photonics Rev. **18** 2301293 (2024).

[7]M.M. Fejer, G.A. Magel, D.H. Jundt, and R.L. Byer, Quasi-phase-matched second harmonic generation: tuning and tolerances, IEEE J. Quantum Electron. **28**, 2631–2654 (1992).

[8]D. Alden, T. Troha, R. Kirste, S. Mita, Q. Guo, A. Hoffmann, M. Zgonik, R. Collazo, and Z. Sitar, Quasi-phase-matched second harmonic generation of UV light using AlN waveguides, Appl. Phys. Lett. **114**, 103504 (2019).

[9]S. Wang, T. Matsushita, T. Matsumoto, S. Yoshida, and T. Kondo, Quasi-phase matched difference frequency generation in corrugation-reduced GaAs/AlGaAs periodically-inverted waveguides, Jpn. J. Appl. Phys. **58**, SBBE01 (2019).

[10]Y. Hayashi, R. Katayama, T. Akiyama, T. Ito, and H. Miyake, Polarity inversion of aluminum nitride by direct wafer bonding, Appl. Phys. Express, **11**, 031003 (2018).

[11]Z. Zhang, Y. Hayashi, T. Tohei, A. Sakai, V. Protasenko, J. Singhal, H. Miyake, H. G. Xing, D. Jena, and Y. Cho, Molecular beam homoepitaxy of N-polar AlN: Enabling role of aluminum-assisted surface cleaning, Sci. Adv. **8**, eabo6408 (2022).

[12]N. Yokoyama, Y. Morioka, T. Murata, H. Honda, K. Serita, H. Murakami, M. Tonouchi, S. Tokita, S. Ichikawa, and Y. Fujiwara, Second harmonic generation in GaN transverse quasi-phase-matched waveguide pumped with femtosecond laser, Appl. Phys. Express **15**, 112002 (2022).

[13]H. Honda, S. Umeda, K. Shojiki, H. Miyake, S. Ichikawa, J. Tatebayashi, Y. Fujiwara, K. Serita, H. Murakami, and M. Tonouchi, 229 nm far-ultraviolet second harmonic generation in a vertical polarity inverted AlN bilayer channel waveguide, Appl. Phys. Express **16**, 062006 (2023).

[14]X. Lu, N. Kumagai, Y. Minami, and T. Kitada, Sublattice reversal in GaAs/Ge/GaAs heterostructures grown on (113)B GaAs substrates, Appl. Phys. Express **11**, 015501 (2018).

[15]S. Koh, T. Kondo, M. Ebihara, T. Ishiwada, H. Sawada, H. Ichinose, I. Shoji, and R. Ito, GaAs/Ge/GaAs sublattice reversal epitaxy on GaAs(100) and (111) substrates for nonlinear optical devices, Jpn. J. Appl. Phys. **38**, L508-L511 (1999).

[16]A. Ohtake, Surface reconstructions on GaAs(001), Surf. Sci. Rep. **63**, 295-327 (2008).

[17]A. Ohtake, N. Ha, and T. Mano, Extremely high- and low- density of Ga droplets on GaAs{111}A, B: surface polarity dependence, Cryst. Growth Des. **15**, 485-488 (2015).

[18]R.D. Bringans, R.I.G. Uhrberg, R.Z. Bachrach, and J.E. Northrup, Arsenic-Terminated Ge(111): An Ideal 1×1 Surface, Phys. Rev. Lett. **55**, 533-536 (1985).

[19]J. Zengenhagen, P.F. Lyman, M. Böhringer, and M.J. Bedzyk, Discommensurate reconstructions of (111)Si and Ge induced by surface alloying with Cu, Ga, and In, phys. stat. sol. **204**, 587-616 (1997).

[20]J.R. Patel, P.E. Freeland, M.S. Hybertsen, D.C. Jacobson, and J.A. Golovchenko, Location of Atoms in the First Monolayer of GaAs on Si, Phys. Rev. Lett. **59**, 2180 (1987).

[21]D.A. Woolf, D.I. Westwood, and R.H. Williams, Surface reconstructions of GaAs(111)A and (111)B: A static surface phase study by reflection high-energy- electron diffraction, Appl. Phys. Lett. **62**, 1370-1372 (1993).

[22]D.A. Woolf, Z. Sobiesierski, D.I. Westwood, and R.H. Williams, The molecular beam epitaxial growth of GaAs/GaAs(111)B: doping and growth temperature studies, J. Appl. Phys. **71**, 4908-4915.

[23]Y. Kajikawa, Y. Son, H. Hayase, H. Ichiba, R. Mori, K. Ushirogouchi, and M. Irie, Suppression of twin generation in the growth of GaAs on Ge(111), J. Cryst. Growth **477**, 40-44 (2017).

[24]D. Pelati, G. Patriarche, O. Mauguin, L. Largeau, L. Tranvers, F. Brisset, G. Glas, and F. Oehler, GaAs(111) epilayers grown by MBE on Ge(111): Twin reduction and polarity, J. Cryst. Growth **519**, 84-90 (2019).

[25]R.D. Bringans, M.A. Olmstead, R.I.G. Uhrberg, and R.Z. Bachrach, Interface formation of GaAs with Si(100), Si(111), and Ge(111): Core-level spectroscopy for monolayer coverages of GaAs, Ga, and As, Phys. Rev. B **36**, 9569-9580 (1987).

[26]S.Y Tong, G. Xu, and W.N. Mei, Vacancy-buckling model for the (2×2) GaAs(111) surface, Phys. Rev. Lett. **52**, 1693-1696 (1984).

[27]A. Ohtake, J. Nakamura, T. Komura, T. Hanada, T. Yao, H. Kuramochi, and M. Ozeki, Surface structure of GaAs{111}A,B-(2×2), Phys. Rev. B **64**, 045318 (2001).

[28]H. Koga, Structure of GaAs($\overline{111}$)under Ga-rich condition: A $\sqrt{19}\times\sqrt{19}$ reconstruction model, Phys. Rev. B **82**, 113301 (2010)